DOI: 10.1002/ejic.200701041

Syntheses, Structures and Magnetic Properties of Dinuclear Copper(II)–Lanthanide(III) Complexes Bridged by 2-Hydroxymethyl-1-methylimidazole

Wei-Xiong Zhang,[a] Yang-Yi Yang,*[a] Shao-Bo Zai,[a] Seik Weng Ng,[b] and Xiao-Ming Chen*[a]

Keywords: Lanthanides / Copper / Nitrogen heterocycles / Magnetic properties

Three discrete dinuclear copper(II)–lanthanide(III) complexes, namely, $[CuLn(mmi)_2(NO_3)_3(H_2O)_2]$ [Ln = La (**1**), Sm (**2**)] and $[CuGd(mmi)_2(NO_3)_2(H_2O)_3][NO_3]$ (**3**) (Hmmi = 2-hydroxymethyl-1-methylimidazole) were synthesized and structurally characterized by X-ray diffraction analysis. In these complexes, dinuclear cores of Cu^{II} and Ln^{III} are consolidated by a pair of μ-1,1-*O* bridges from mmi at a distance of 3.36–3.46 Å. The temperature dependence of the magnetic susceptibility and the field dependence of the magnetization indicate that **1**, **2** and **3** exhibit paramagnetic, antiferromagnetic and ferromagnetic behaviours, respectively. The value of the J_{Cu-Gd} coupling constant of **3** [8.7(1) cm^{-1}] is fairly large, which is probably related to the small dihedral angles, *α* (5.0°), between the two planes of O–Cu–O and O–Gd–O in the CuO_2Gd core.

Introduction

Since 1985, the magnetic behaviour of heteronuclear complexes containing both lanthanide [abbreviated as Ln^{III} hereafter] and transition-metal ions has attracted increasing interest for their potential application in material science.[1] One interesting aspect is the Gd^{III}–Cu^{II} magnetic exchange interaction, which displays magnetic properties that are amenable to rather simple analysis, as Gd^{III} with an $S = 7/2$ single-ion ground state does not possess a first-order orbital moment. Several polynuclear complexes[1–5] involving Gd^{III} and Cu^{II} ions were shown to exhibit overall ferromagnetic behaviours. Recent studies on perfectly isolated dinuclear species have demonstrated that ferromagnetism is an intrinsic property of the Gd^{III}–Cu^{II} pair.[6–8]

We reported a number of heteronuclear Cu–Ln complexes bridged by carboxylate groups,[9,10] all of which dominate weakly magnetic exchange between Cu^{II} and Ln^{III}. Because the magnitude of magnetic interaction is exponentially dependent on the Cu–Gd distance,[11] and the distances of Cu^{II} and Ln^{III} bridged by μ-*O*,*O*′ carboxylate groups are rather long; therefore, the search for other bridging ligands that may shorten the distance of the Cu–Ln bond is one of the important tasks in the synthesis of 3d–4f heteronuclear complexes. 2-Hydroxymethyl-1-methylimidazole (Hmmi)[12] is a mixed-atom donor ligand, which can chelate to a transition-metal ion through both the N and O atoms, whereas the O atom may further ligate to another metal ion. By treating Hmmi with Cu^{II}, we synthesized a series of homometallic cupric complexes, including mononuclear, dinuclear and tetranuclear complexes,[13] and all of them exhibited chelation of both the N and O atoms of the mmi ligand to the copper ions. Encouraged by this interesting result, and the fact that the hard-donor O atom tends to bind oxophilic lanthanide centres and the soft-donor N atom tends to bind to transition-metal centres, we used the mixed donor ligand (Hmmi) to bridge the Cu^{II} and Ln^{III} centres. As was expected, the synthesis of several dinuclear Cu–Ln complexes was successful. Herein, we report the preparation, structure and magnetic properties of $[CuLn(mmi)_2(NO_3)_3(H_2O)_2]$ [Ln = La (**1**), Sm (**2**)] and $[CuGd(mmi)_2(NO_3)_2(H_2O)_3][NO_3]$ (**3**). The synthetic strategy is shown in Scheme 1. A 4:1 reactant ratio of Ln^{III}/Cu^{II} was used, as the reaction yield was very low if a stoichio-

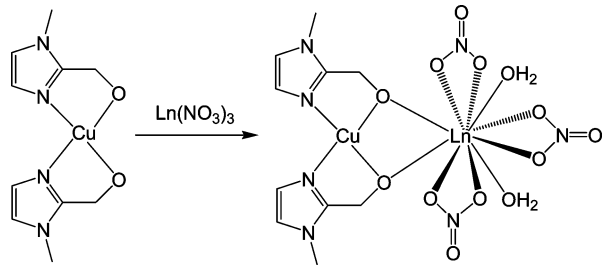

Scheme 1. Synthetic strategy.

[a] MOE Key Laboratory of Bioinorganic and Synthetic Chemistry, School of Chemistry and Chemical Engineering, Sun Yat-Sen University,
Guangzhou 510275, China
Fax: +86-20-8411-2245
E-mail: cesyyy@mail.sysu.edu.cn
cxm@mail.sysu.edu.cn
[b] Institute of Postgraduate Studies and Research, University of Malaya,
50603 Kuala Lumpur, Malaysia

metric ratio (1:1) was used, probably because the Cu atom chelated by both the N and O atoms of the mmi ligand has more stability than the Ln bridged by an O atom.

Results and Discussion

Crystal Structures

[CuLa(mmi)$_2$(NO$_3$)$_3$(H$_2$O)$_2$] (1)

The crystal structure of **1** consists of a discrete dinuclear [CuLa(mmi)$_2$(NO$_3$)$_3$(H$_2$O)$_2$] molecule (Figure 1a). Two mmi ligands coordinate to the Cu^{II} atom at a twofold axial symmetry, and each of the mmi ligands chelates to the Cu^{II} centre by a nitrogen atom [Cu–N 1.965(6) Å] and an oxygen atom [Cu–O 1.938(5) Å] (Table 1). The two hydroxy oxygen atoms also ligate to a La^{III} ion, which results in a dinuclear Cu–La core joined by a pair of μ-1,1-*O* bridges. The coordination environment of the Cu^{II} atom is a square-planar geometry. Besides two bridging oxygen atoms [La–O 2.427(4) Å], the La^{III} ion is ligated by three chelated nitrate anions [La–O 2.624(5)–2.737(6) Å], as well as two aqua ligands [La–O 2.631(5) Å]; the coordination polyhedron about the La^{III} ion can be described as a ten coordination distorted dicapped square-antiprismatic geometry (Figure 1b). The two cap position atoms [O(3), O(3A)] are the most distant atoms (2.737 Å) from La^{III} centre.

There is a twofold axis passing through the Cu^{II} and La^{III} ions in the dinuclear Cu–La core; thus, the four-membered CuO$_2$La ring is strictly coplanar, and the La–O–Cu bond angle is 104.3(2)°, whereas those of O–La–O and O–Cu–O are 65.7(2)° and 85.6(3)°, respectively. The Cu^{II}···La^{III} separation of 3.4601(1) Å is reasonable.[6–8] Other known dinuclear Cu–Ln compounds are usually bridged by phenolato groups of Schiff bases, and their synthetic strategy was first to trap a Cu^{II} ion into a cavity of a phenolic Schiff base consisting of a N$_2$O$_2$ donor set, which

Table 1. Selected bond lengths and angles for **1** and **2**.[a]

Bond lengths [Å] or angles [°]	**1**	**2**
Ln(1)···Cu(1)	3.4601(1)	3.4442(2)
Ln(1)–O(1)	2.427(4)	2.419(4)
Ln(1)–O(2)	2.624(5)	2.625(5)
Ln(1)–O(1W)	2.631(5)	2.621(4)
Ln(1)–O(2A)	2.624(5)	2.625(5)
Ln(1)–O(5)	2.719(4)	2.703(4)
Ln(1)–O(3)	2.737(6)	2.738(5)
Cu(1)–O(1)	1.938(5)	1.937(4)
Cu(1)–N(1)	1.965(6)	1.949(4)
O(1A)–Ln(1)–O(1)	65.7(2)	66.16(2)
O(1W)–Ln(1)–O(3)	106.33(2)	106.50(1)
O(5)–Ln(1)–O(3A)	109.10(1)	109.21(1)
O(1)–Ln(1)–O(3)	112.63(2)	112.64(1)
O(2)–Ln(1)–O(1WA)	118.93(2)	118.94(1)
O(2)–Ln(1)–O(5A)	120.57(2)	120.57(1)
O(2)–Ln(1)–O(3A)	134.04(2)	133.75(1)
O(1)–Ln(1)–O(5A)	134.63(2)	134.49(1)
O(1)–Ln(1)–O(1WA)	138.87(2)	139.55(1)
O(1W)–Ln(1)–O(1WA)	141.7(2)	140.93(2)
O(1)–Ln(1)–O(5)	147.06(1)	146.62(1)
O(2)–Ln(1)–O(2A)	160.8(2)	161.2(2)
O(3)–Ln(1)–O(3A)	174.64(2)	174.7(2)
O(5A)–Ln(1)–O(5)	46.80(2)	47.16(2)
O(2)–Ln(1)–O(3)	47.19(2)	47.45(1)
O(5)–Ln(1)–O(3)	65.60(1)	65.50(1)
O(2)–Ln(1)–O(1W)	68.01(2)	67.99(1)
O(1W)–Ln(1)–O(5)	71.38(2)	71.00(1)
O(1W)–Ln(1)–O(3A)	71.83(1)	71.63(1)
O(1)–Ln(1)–O(3A)	72.17(1)	72.13(1)
O(1W)–Ln(1)–O(5A)	73.57(1)	73.30(1)
O(2)–Ln(1)–O(5)	78.27(1)	77.92(1)
O(1)–Ln(1)–O(1W)	78.34(2)	78.42(1)
O(1)–Ln(1)–O(2)	78.64(2)	78.49(2)
O(1A)–Ln(1)–O(1W)	138.87(2)	139.55(1)
O(1)–Ln(1)–O(2A)	85.27(2)	85.75(1)
O(1A)–Cu(1)–N(1A)	84.2(2)	84.47(2)
N(1)–Cu(1)–N(1A)	106.0(3)	105.2(3)
O(1)–Cu(1)–N(1A)	169.7(2)	170.23(2)
O(1)–Cu(1)–O(1A)	85.6(3)	85.9(2)
O(1)–Cu(1)–N(1)	84.2(2)	84.47(2)

[a] Symmetry code: A: –*x*, *y*, –*z* + 1/2.

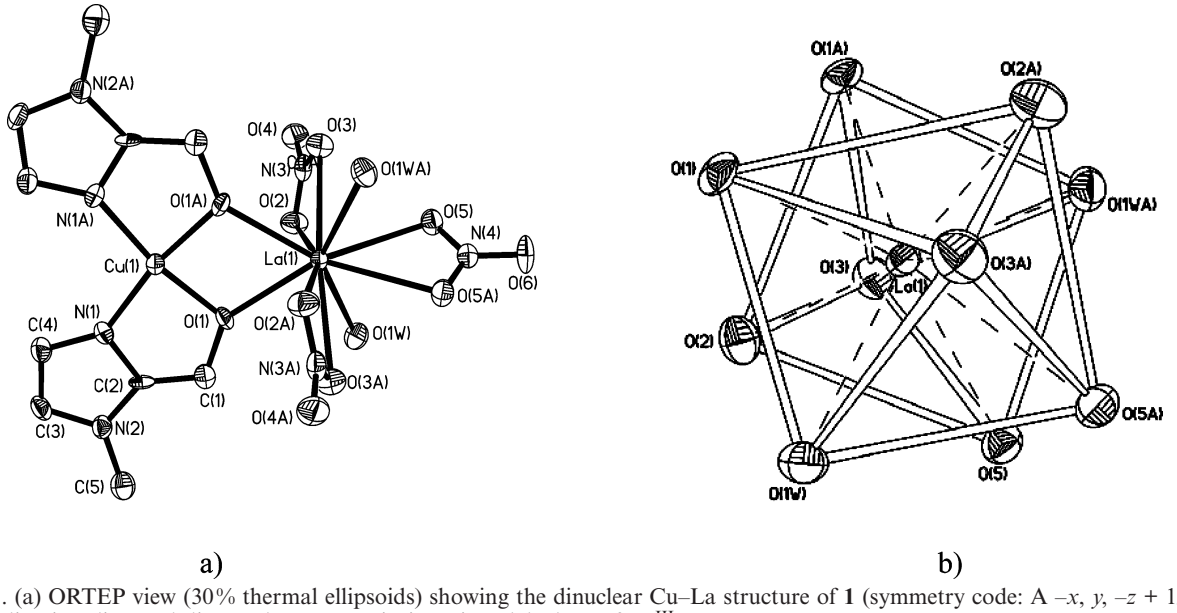

a) b)

Figure 1. (a) ORTEP view (30% thermal ellipsoids) showing the dinuclear Cu–La structure of **1** (symmetry code: A –*x*, *y*, –*z* + 1/2.); (b) ten coordination distorted dicapped square-antiprismatic polyhedron of La^{III}.

was then used as a metalloligand to ligate the lanthanide metal by the two phenolato oxygen atoms. As the four atoms of the N_2O_2 donor set in the Schiff base compounds are not in a plane, the dinuclear CuO_2Ln cores are always not coplanar.[6,8]

[CuSm(imm)$_2$(NO$_3$)$_3$(H$_2$O)$_2$] (2)

The crystal structure of **2** is isomorphous to that of **1**, and only very small metric differences were observed for the two complexes. As a result of the lanthanide contraction, the metal–ligand bonds in **2** are slightly shorter than the corresponding ones in **1**, and they are compared in Table 1; however, the bond angles in both **1** and **2** are almost the same.

[CuGd(imm)$_2$(NO$_3$)$_2$(H$_2$O)$_3$][NO$_3$] (3)

Complex **3** consists of a discrete dinuclear Cu–Gd cation (Figure 2a) and a nitrate anion. Similarly to those in **1**, the two mmi ligands chelate to the Cu^{II} ion by nitrogen atoms [Cu-N 1.948(5), 1.966(5) Å] and oxygen atoms [Cu-O 1.932(4), 1.933(4) Å] (Table 2), whereas the two oxygen atoms also bind to the Gd^{III} ion to form two μ-1,1-*O* bridges, which results in a dinuclear Cu–Gd core. The Cu^{II} ion features a square-planar coordination geometry. Besides the two bridging oxygen atoms [Gd–O 2.339(4), 2.308(4) Å], the Gd^{III} ions are also ligated by two chelated nitrate anions [Gd–O 2.517(5)–2.604(5) Å], as well as three aqua ligands [Gd–O 2.428(4)–2.436(5) Å] to furnish a nine coordination distorted monocapped square-antiprism geometry (Figure 2b) with O(7) occupying the cap position. The structural difference between **1** (or **2**) and **3** can be attributed to the smaller ionic radius of Gd^{III} relative to that of La^{III} [or Sm^{III}], which leads to the smaller coordination number in **3**.

Table 2. Selected bond lengths [Å] and angles [°] for **3**.

Gd(1)···Cu(1)	3.366(2)	Gd(1)–O(1W)	2.435(4)
Gd(1)–O(2)	2.308(4)	Gd(1)–O(2W)	2.436(5)
Gd(1)–O(1)	2.339(4)	Gd(1)–O(3W)	2.428(4)
Gd(1)–O(4)	2.517(5)	Cu(1)–O(1)	1.932(4)
Gd(1)–O(6)	2.539(5)	Cu(1)–O(2)	1.933(4)
Gd(1)–O(3)	2.598(5)	Cu(1)–N(3)	1.948(5)
Gd(1)–O(7)	2.604(5)	Cu(1)–N(1)	1.966(5)
O(2)–Gd(1)–O(1)	67.54(1)	O(1)–Cu(1)–O(2)	83.87(2)
O(2)–Gd(1)–O(3W)	130.49(1)	O(1)–Cu(1)–N(3)	167.7(2)
O(1)–Gd(1)–O(3W)	73.82(1)	O(2)–Cu(1)–N(3)	83.98(2)
O(2)–Gd(1)–O(1W)	149.91(1)	O(1)–Cu(1)–N(1)	84.80(2)
O(1)–Gd(1)–O(1W)	142.17(1)	O(2)–Cu(1)–N(1)	168.12(2)
O(3W)–Gd(1)–O(1W)	71.80(1)	N(3)–Cu(1)–N(1)	107.4(2)
O(2)–Gd(1)–O(2W)	80.52(2)	O(6)–Gd(1)–O(3)	136.76(2)
O(1)–Gd(1)–O(2W)	90.77(1)	O(2)–Gd(1)–O(7)	81.55(2)
O(3W)–Gd(1)–O(2W)	70.07(2)	O(1)–Gd(1)–O(7)	77.16(2)
O(1W)–Gd(1)–O(2W)	92.05(2)	O(3W)–Gd(1)–O(7)	118.86(2)
O(2)–Gd(1)–O(4)	81.65(1)	O(1W)–Gd(1)–O(7)	106.35(2)
O(1)–Gd(1)–O(4)	133.38(1)	O(2W)–Gd(1)–O(7)	161.20(2)
O(3W)–Gd(1)–O(4)	147.46(1)	O(4)–Gd(1)–O(3)	49.86(1)
O(1W)–Gd(1)–O(4)	76.42(1)	O(4)–Gd(1)–O(7)	63.98(2)
O(2W)–Gd(1)–O(4)	118.51(2)	O(6)–Gd(1)–O(7)	49.73(1)
O(2)–Gd(1)–O(6)	126.23(1)	O(3)–Gd(1)–O(7)	112.09(2)
O(1)–Gd(1)–O(6)	79.17(1)	O(2)–Gd(1)–N(5)	79.81(1)
O(3W)–Gd(1)–O(6)	72.48(1)	O(1)–Gd(1)–N(5)	145.72(1)
O(1W)–Gd(1)–O(6)	75.88(1)	O(3W)–Gd(1)–N(5)	139.26(2)
O(2W)–Gd(1)–O(6)	142.55(2)	O(1W)–Gd(1)–N(5)	71.61(2)
O(4)–Gd(1)–O(6)	93.32(1)	O(2W)–Gd(1)–N(5)	93.99(1)
O(2)–Gd(1)–O(3)	76.18(1)	O(4)–Gd(1)–N(5)	24.80(1)
O(1)–Gd(1)–O(3)	140.90(2)	O(6)–Gd(1)–N(5)	114.55(2)
O(3W)–Gd(1)–O(3)	124.37(1)	O(3)–Gd(1)–N(5)	25.21(2)
O(1W)–Gd(1)–O(3)	73.95(2)	O(7)–Gd(1)–N(5)	88.34(2)
O(2W)–Gd(1)–O(3)	68.79(2)		

The four-membered CuO_2Gd core of **3** is basically planar, and the mean deviation from the least-squares plane is 0.035 Å. The deviations of each atom from the least-

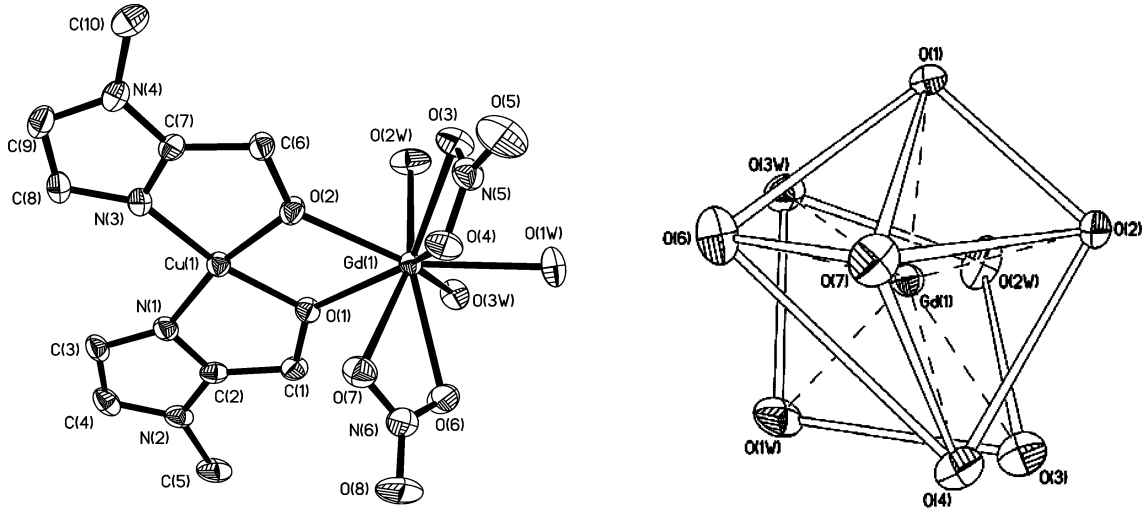

Figure 2. (a) ORTEP view (30% thermal ellipsoids) showing the dinuclear Cu–Gd structure of **3**; (b) nine coordination distorted monocapped square-antiprism polyhedron of Gd^{III}.

squares plane are 0.0301(3) Å for Gd(1), 0.0405(3) Å for Cu(1), 0.0350(4) Å for O(1) and 0.0356(4) Å for O(2), and the dihedral angle between the O(1)–Cu–O(2) and O(1)–Gd–O(2) planes is 5.0°. The Cu(1)–O(1)–Gd(1), Cu(1)–O(2)–Gd(1), O(1)–Cu(1)–O(2) and O(2)–Gd(1)–O(1) bond angles are 103.6(1), 104.7(2), 83.9(2) and 67.5(1)°, respectively. The separation between the Cu^{II} and Gd^{III} atoms [3.366(2) Å] is very similar to those (3.24–3.53 Å) in the dinuclear Cu–Gd compounds bridged by phenolato polydental Schiff bases.[6,8]

Magnetic Properties

La^{III} is a diamagnetic ion; thus, **1** is expected to be a paramagnet because Cu^{II} is in a $3d^9$ state. At room temperature, the $\chi_m T$ product for **1** is 0.40 $cm^3 mol^{-1} K$, which is close to the expected value (0.375 $cm^3 mol^{-1}$ K, g = 2.0) for one Cu^{II} ion, and it remains constant at temperatures above 8 K and then decreases to 0.35 $cm^3 mol^{-1} K$ at 2 K (Figure 3) probably as a result of the very weak antiferromagnetic interaction between the dinuclear molecules. The magnetization versus field curve of **1** at 2.0 K compares well with the Brillouin function for an S = 1/2 spin (Figure 4), which further indicates that **1** is a paramagnet.

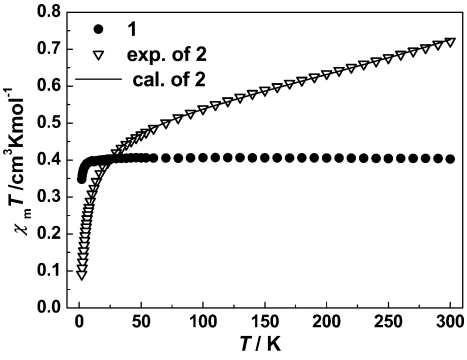

Figure 3. $\chi_m T$ vs. T plots for **1** (dot) and **2** (experimental: triangle; calculated: solid line).

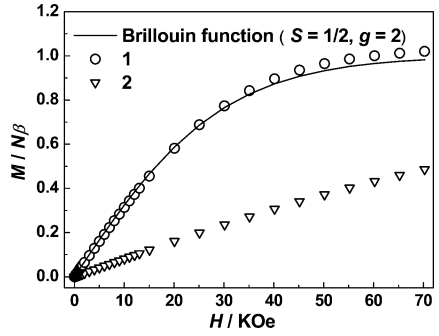

Figure 4. Field dependence of the magnetization at 2 K for **1** (circle) and **2** (triangle). The solid line represents the Brillouin function for the S = 1/2 spin.

The ^6H ground term for Sm^{III} is split by spin-orbit coupling into six Stark sublevels; the excited states can be populated at room temperature but the ground state $^6H_{5/2}$ will be only populated at low temperatures. Therefore, the expected $\chi_m T$ value for Sm^{III} will decrease when the temperature is lowered, and it is about 0.1 $cm^3 mol^{-1}$ K [$(\chi_m T)_{LT} = N\beta^2 g^2 J(J + 1)/3k$] at 2 K.[14] Considering the contribution of the Cu^{II} ion, the $\chi_m T$ value expected for **2** is about 0.5 $cm^3 mol^{-1} K$ at 2 K if the Cu^{II} and Sm^{III} ions are not interacting. However, the $\chi_m T$ value of **2** at 2 K is only 0.08 $cm^3 mol^{-1}$ K, which indicates that antiferromagnetic exchange interactions occur between the Sm^{III} and Cu^{II} ions. The magnetization of **2** is only 0.49 $N\beta$ at 2.0 K with a field up to 70 kOe. This value is much lower than the simulated value (1.43 $N\beta$ at 70 kOe) calculated with the Brillouin function for one Cu^{II} ion and one Sm^{III} ion, which do not interact; this further indicates that **2** behaves as an antiferromagnet. Unfortunately, the quantitative description of the magnetic properties of Sm^{III}-containing heterometallic complexes is not an easy task because of the ligand-field effect and spin-orbit coupling of the Sm^{III} ion.[15] To estimate the magnitude of the exchange interaction between the Sm^{III} and Cu^{II} ions, we attempted to simulate roughly the magnetic behaviour of **2** with the following process.

For the Sm^{III} ion, by taking the energy of the ground state as the origin, the energies $E(J)$ increase from $^6H_{5/2}$ to $^6H_{15/2}$, and they can be calculated from: $E(J) = \lambda[J(J + 1) - 35/4]/2$, where λ is the spin-orbit coupling parameter. Therefore, the molar magnetic susceptibility of Sm^{III} can be presented as Equations (1), (2) and (3).[14]

$$\chi_{Sm} = \frac{\sum_{J=5/2}^{15/2}(2J+1)\chi(J)\exp[-E(J)/kT]}{\sum_{J=5/2}^{15/2}\chi(J)\exp[-E(J)/kT]} \quad (1)$$

$$\chi(J) = \frac{Ng_J^2\beta^2 J(J+1)}{3kT} + \frac{2N\beta^2(g_J-1)(g_J-2)}{3\lambda} \quad (2)$$

$$g_J = \frac{3}{2} + \frac{S(S+1)-L(L+1)}{2J(J+1)} \quad (3)$$

where S, L and J represent the spin, orbital and total angular momentum quantum number, respectively. N is Avogadro's number, β is the Bohr magneton, g_J is the Zeeman factor and k is the Boltzmann constant. Considering the paramagnetic behaviour of the Cu^{II} ion and the antiferromagnetic exchange between the Sm^{III} and Cu^{II} ions, the magnetic susceptibility of **2** was derived as Equation (4).

$$\chi_m = \frac{\chi_{Sm}T + N\beta^2 g_{Cu}^2 S_{Cu}(S_{Cu}+1)/3k}{T-\theta} \quad (4)$$

A correction term, θ, was included in this equation to account for the exchange interaction occurring between the Sm^{III} and Cu^{II} ions. To avoid deviation of Equation (4) by the magnetic interactions between the dinuclear cores, only data above 9 K were fitted by the least-squares method,

which led to the following reasonable parameters: g_{Cu} = 2.08(1), λ = 276(2) cm^{-1}, θ = –6.97(9) K and residual factor $R = 1.8 \times 10^{-5}$ ($R = [\Sigma(\chi_{obs}T - \chi_{calcd}T)^2/\Sigma(\chi_{obs}T)^2]$). The spin-orbit coupling parameter λ observed is very close to the typical value of the order of 200 cm^{-1} for Sm^{III}.[14b] A negative value of θ indicated the distinct antiferromagnetic nature between the Sm^{III} and Cu^{II} ions in **2**, which was reported in other Sm^{III}–Cu^{II} systems previously.[15,16] The correction term θ was not used before to investigate the magnitude of exchange interaction between the Sm^{III} and Cu^{II} ions, which precludes its comparison with those of the other known Sm^{III}–Cu^{II} exchange systems. However, it may provide new data for the investigation in Sm^{III}–Cu^{II} exchange systems in the future.

For **3**, the $\chi_m T$ product is 8.6 $cm^3 mol^{-1} K$ at room temperature, which is slightly larger than the expected value (8.25 $cm^3 mol^{-1}$ K) for noninteracting Cu^{II} and Gd^{III} ions. By lowering the temperature, a gradual increase in $\chi_m T$ was observed, and the value reached 10.13 $cm^3 mol^{-1} K$ at 9 K (Figure 5). This behaviour reveals a ferromagnetic coupling between S = 1/2 and S = 7/2, which was further confirmed by the field-dependent magnetization curve of **3** at 2 K. The decrease in $\chi_m T$ at lower temperatures is due to the weak antiferromagnetic interaction between the resulting S = 4 spin.

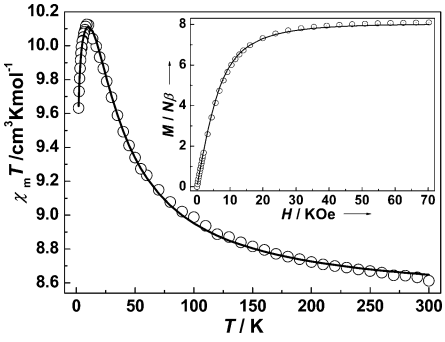

Figure 5. $\chi_m T$ vs. T plots for **3** (experimental: cycle; calculated: solid line). Inset: Field dependence of the magnetization at 2 K for **3** (the solid line represents the Brillouin function for the S = 4 spin).

Gd^{III} is a $4f^7$ ion with $^8S_{7/2}$ ground state without orbital contribution; thus, a simple Heisenberg–Dirack–van Vleck phenomenological spin exchange Hamiltonian, $H = -J_{Cu-Gd}S_{Cu}S_{Gd}$, can be applied to the magnetic study of this Gd^{III}–Cu^{II} system. By taking into account the intermolecular interaction (J'), a theoretical expression of susceptibility is presented as Equations (5) and (6).[6g]

$$\chi_m = \frac{4N\beta^2 TF_d}{kT - J'F_d} \quad (5)$$

$$F_d = \frac{15g_4^2 + 7g_3^2 \exp(-4J_{Cu-Gd}/kT)}{9 + 7\exp(-4J_{Cu-Gd}/kT)} \quad (6)$$

where $g_3 = (9g_{Gd} - g_{Cu})/8$ and $g_4 = (7g_{Gd} + g_{Cu})/8$. Least-squares fitting of the experimental data led to the following set of parameters (Figure 5): g_{Cu} = 2.06(1), g_{Gd} = 2.03(1), J_{Cu-Gd} = 8.7(1) cm^{-1}, J' = –0.013(1) cm^{-1} and residual factor $R = 2.9 \times 10^{-6}$ [$R = \{\Sigma(\chi_{obs}T - \chi_{calcd}T)^2/\Sigma(\chi_{obs}T)^2\}$]. For the systems with a CuO_2Gd fragment,[6–8] the magnitude of J_{Cu-Gd} is a function of the dihedral angle (α) between the O–Cu–O and O–Gd–O planes, which was suggested by Kahn[2d] and proposed by Costes with an exponential relationship: $|J_{Cu-Gd}| = 11.5\exp(-0.054\alpha)$.[6d] The experimental values of 8.7(1) cm^{-1} is very close to the value calculated with this correlation of 8.79 cm^{-1} for **3** (α = 5.0°). A comparison of the dihedral angles (α) and magnetic parameters (J_{Cu-Gd}) for the CuO_2Gd core structures reported in the literature are listed in Table 3. This magnetostructural correlation indicated that the decrease in the dihedral angle α between the O–Cu–O and O–Gd–O planes may contribute to the increase in the interaction parameter J_{Cu-Gd} when α changes from 47 to 1.7°.

Table 3. Comparative values of J and the dihedral angle (α) for various dinuclear Cu^{II}–Gd^{III} complexes with a CuO_2Gd bridging core.

Formula	J [cm^{-1}]	α [°]	Ref.
$Gd(hfa)_3Cu(salen)$	0.4	47.1	[2d]
$Cu(salabza)Gd(hfac)_3$	0.8	47.4	[8e]
$Cu(salen)Gd(pta)_3$	1.21	33.1	[8c]
$Cu(acacen)Gd(hfa)_3$	1.25	39	[8c]
$Gd(hfa)_3Cu(salen)(Meim)$	1.42	39.6	[2d]
$Cu(acacen)Gd(pta)_3$	1.47	41.4	[8c]
$[CuGd(ems)(NO_3)_3H_2O]Cu(ems)$	1.88	24.5	[8d]
$CuGd(hmp)_2(NO_3)_3(H_2O)_2$	3.36	20.5	[7a]
$LCu(O_2COMe)Gd(thd)_2$	3.5	19.1	[6c]
$LCuGd(O_2CCF_3)_3(C_2H_5OH)_2$	4.42	13.6	[6g]
$[(3\text{-}MeOsalamo)CuGd(OAc)_3]$	4.5	20.1	[8b]
$LCu(C_3H_6O)Gd(NO_3)_3$	4.8	16.7	[6b]
$LCuGd(NO_3)_3$	4.98	18.9	[6e]
$[CuL_2Gd(NO_3)_3]$	5.4	7.1	[8a]
$LCu(MeOH)Gd(NO_3)_3$	6.8	12.5	[6b]
$LCuGd(NO_3)_3(Me_2CO)$	7.0	12.9	[6a]
$[(3\text{-}MeOsalamo)CuGd(NO_3)_3]$	7.6	9.3, 13.6	[8b]
$[CuGd(imm)_2(NO_3)_2(H_2O)_3][NO_3]$	8.7	5.0	this work
$[LCuCl_2Gd(H_2O)_4]Cl{\cdot}2H_2O$	10.1	1.7	[6d]

Conclusions

Three dinuclear, hydroxy-bridged Cu–Ln complexes were successfully prepared, and their magnetic properties were studied. These complexes have similar structural features; however, their magnetic properties are very different because of the presence of different lanthanide ions. With the diamagnetic La^{III} ion, complex **1** behaves as a paramagnet of the Cu^{II} ion. Sm^{III}, with a ^6H ground term, exhibits antiferromagnetic coupling with Cu^{II}, which leads to an antiferromagnet in **2**, whereas in **3**, ferromagnetic coupling is observed between the Gd^{III} and Cu^{II} ions and a very strong J_{Cu-Gd} coupling constant of 8.7(1) cm^{-1} was exhibited, which is related to the small dihedral angle α (5.0°) between the O–Cu–O and O–Gd–O planes.

Table 4. Crystallographic data for complexes **1**, **2** and **3**.

Complex	**1**	**2**	**3**
Formula	$C_{10}H_{18}CuLaN_7O_{13}$	$C_{10}H_{18}CuN_7O_{13}Sm$	$C_{10}H_{20}CuGdN_7O_{14}$
Formula weight	646.74	658.20	683.12
Crystal system	monoclinic	monoclinic	monoclinic
Space group	*C*2/*c* (No.15)	*C*2/*c* (No.15)	$P2_1/c$ (No.14)
Temperature [K]	293(2)	293(2)	293(2)
a [Å]	17.550(5)	17.441(4)	6.985(4)
b [Å]	16.406(4)	16.314(4)	11.773(6)
c [Å]	7.373(2)	7.359(4)	25.83(1)
β [°]	108.00(1)	107.87(2)	91.93(1)
V [Å^3]	2019.0(9)	1992.9(1)	2123(2)
Z	4	4	4
$D_{calcd.}$ [g cm^{-3}]	2.128	2.194	2.137
μ.[mm^{-1}]	3.223	4.068	4.183
F(000)	1268	1288	1336
Crystal size [mm]	0.40 × 0.25 × 0.15	0.40 × 0.35 × 0.30	0.30 × 0.30 × 0.10
Crystal colour and habit	Deep blue block	Deep blue block	Deep blue block
θ range [°]	2.27 to 27.46	2.50 to 29.00	2.34 to 27.00
Reflections collected	1488	2715	5004
Independent reflections	1339 (R_{int} = 0.0317)	2636 (R_{int} = 0.0284)	4625 (R_{int} = 0.0470)
Transmission factors	0.769/0.642	0.944/0.516	0.968/0.446
Parameters refined	144	148	299
Goodness-of-fit on F^2	1.108	1.084	1.035
$R_1/wR_2[I > 2\sigma(I)]$[a]	0.0342/0.0934	0.0442/0.1174	0.0417/0.0894
R_1/wR_2 (all data)[a]	0.0381/0.0965	0.0480/0.1205	0.0629/0.0974
Largest diff. peak and hole [e Å^{-3}]	0.740/–0.831	1.561/–1.463	1.020/–0.705

[a] $R_1 = \Sigma||F_o| - |F_c||/\Sigma|F_o|$, $wR_2 = [\Sigma w(|F_o| - |F_c|)^2/\Sigma w|F_o|^2]^{1/2}$.

Experimental Section

Hmmi was synthesized by a slightly modified literature method.[12] The lanthanide(III) nitrates were converted from their oxides by nitric acid. Other reagents were commercially available and used as received. The C, H and N microanalyses were carried out with an Elementar Vario EL analyzer. The FTIR spectra were recorded from KBr pellets in range 4000–400 cm^{-1} with a Nicolet 5DX spectrometer. The magnetic measurements were performed on polycrystalline samples with a Quantum Design MPMS XL-7 SQUID magnetometer in the temperature range 2–300 K. Diamagnetic corrections were estimated from Pascal's constant.[14b]

[CuLa(mmi)$_2$(NO$_3$)$_3$(H$_2$O)$_2$] (1): To a solution of Hmmi (0.112 g, 1 mmol) dissolved in methanol (4 cm^3) was added sodium hydroxide (1.5 mmol), and the solution was vigorously stirred for 10 min. A solution of $Cu(NO_3)_2{\cdot}3H_2O$ (0.121 g, 0.5 mmol) in methanol (4 cm^3) and aqua $La(NO_3)_3{\cdot}6H_2O$ (0.866 g, 2 mmol, 1 cm^3) was then added, and the mixture was stirred for 10 min. The resulting blue solution was adjusted to pH = 5.4 by the addition of nitric acid or sodium hydroxide. The solution was then stored at room temperature for about 10 d to yield deep-blue block crystals (0.129 g, ca. 40% yield base on Hmmi). IR (KBr): $\tilde{\nu}$ = ca. 3382 (s, br) (ν_{OH} of water), 1633 (m) ($\nu_{C=N}$), 1074 (m) (δ_{C-O}) cm^{-1}. $C_{10}H_{18}CuLaN_7O_{13}$ (646.74): calcd. C 18.57, H 2.81, N 15.16; found C 18.38, H 2.92, N 15.10.

[CuSm(mmi)$_2$(NO$_3$)$_3$(H$_2$O)$_2$] (2): Deep-blue crystals of **2** (ca. 40% yield) were prepared according to the procedure used for **1** by using $Sm(NO_3)_3{\cdot}6H_2O$ instead of $La(NO_3)_3{\cdot}6H_2O$. IR data is identical to that of **1**. $C_{10}H_{18}CuN_7O_{13}Sm$ (658.20): calcd. C 18.25, H 2.76, N 14.90; found C 18.08, H 2.72, N 15.01.

[CuGd(mmi)$_2$(NO$_3$)$_2$(H$_2$O)$_3$][NO$_3$] (3): Deep-blue crystals of **3** (ca. 50% yield) were prepared according to the procedure used for **1** by using $Gd(NO_3)_3{\cdot}6H_2O$ instead of $La(NO_3)_3{\cdot}6H_2O$. IR (KBr): $\tilde{\nu}$ = ca. 3360 (s, br) (ν_{OH} of water), 1632 (m) ($\nu_{C=N}$), 1297–1449 (ν_{N-O} of noncoordinated NO^{3-} anions involved in hydrogen bonds), 1083 (m) (δ_{C-O}) cm^{-1}. $C_{10}H_{20}CuGdN_7O_{14}$ (683.12): calcd. C 17.58, H 2.95, N 14.35; found C 17.39, H 2.76, N 14.10.

X-ray Crystallography: A summary of selected crystallographic data for **1**–**3** is given in Table 4. The data collections were carried out with a Siemens R3m diffractometer by using graphite-monochromated Mo-K_α (λ = 0.71073 Å) radiation at 293(2) K.

For each complex, determination of the crystal class, orientation matrix and cell dimensions were performed according to the established procedures. The intensity data were collected by using the ω-scan mode. Absorption corrections were applied by fitting a pseudoellipsoid to the ψ-scan data of selected strong reflections over a range of 2θ angles.[17]

Most of the non-hydrogen atoms in each crystal structure were located with the direct methods and subsequent Fourier syntheses were employed to recover the remaining non-hydrogen atoms.[18] All non-hydrogen atoms were refined anisotropically. All the hydrogen atoms were held stationary and included in the final stage of full-matrix least-squares refinement based on F^2 by using the SHELXL-97 program package.[19] Analytical expressions of the neutral-atom scattering factors were employed and anomalous dispersion corrections were incorporated.[20] Selected bond lengths and bond angles are listed in Tables 1 and 2. CCDC-654391 (for **1**), -654392 (for **2**) and -654393 (for **3**) contain the supplementary crystallographic data for this paper. These data can be obtained free of charge from The Cambridge Crystallographic Data Centre via www.ccdc.cam.ac.uk/data_request/cif.

Acknowledgments

The authors acknowledge financial support by the Natural Science Foundation of China (50572125), MOST (2007CB815302) and

Guangdong Natural Science Foundation (04205405). We also thank the Chemistry Department of the Chinese University of Hong Kong for donation of the diffractometer.

[1] A. Bencini, C. Benelli, A. Caneschi, R. L. Carlin, A. Dei, D. Gatteschi, *J. Am. Chem. Soc.* **1985**, *107*, 8128–8136.

[2] a) C. Benelli, A. Caneschi, D. Gatteschi, O. Guillou, L. Pardi, *Inorg. Chem.* **1990**, *29*, 1750–1755; b) M. Andruh, O. Kahn, J. Sainto, Y. Dromzee, S. Jeannin, *Inorg. Chem.* **1993**, *32*, 1623–1628; c) M. Andruh, I. Ramade, E. Codjovi, O. Guillou, O. Kahn, J. C. Trombe, *J. Am. Chem. Soc.* **1993**, *115*, 1822–1829; d) I. Ramade, O. Kahn, Y. Jeannin, F. Robert, *Inorg. Chem.* **1997**, *36*, 930–936.

[3] a) A. J. Blake, P. E. Y. Milne, P. Thornton, R. E. P. Winpenny, *Angew. Chem. Int. Ed. Engl.* **1991**, *30*, 1139–1141; b) C. Benelli, A. J. Blake, P. E. Y. Milne, J. M. Rawson, R. E. P. Winpenny, *Chem. Eur. J.* **1995**, *1*, 614–618; c) C. Benelli, A. J. Blake, P. E. Y. Milne, J. M. Rawson, R. E. P. Winpenny, *J. Chem. Soc. Dalton Trans.* **1999**, 4125–4126.

[4] a) R. Koner, H.-H. Lin, H.-H. Wei, S. Mohanta, *Inorg. Chem.* **2005**, *44*, 3524–3536; b) J.-P. Costes, F. Dahan, A. Dupuis, D. Bruno, G.-T. Javier, J.-P. Laurent, *Eur. J. Inorg. Chem.* **2001**, 363–365; c) N. Sakagami, M. Tsunekawa, T. Konno, K. Okamoto, *Chem. Lett.* **1997**, 575–576.

[5] a) Q.-D. Liu, S. Gao, J.-R. Li, Q.-Z. Zhou, K.-B. Yu, B.-Q. Ma, S.-W. Zhang, X.-X. Zhang, T.-Z. Jin, *Inorg. Chem.* **2000**, *39*, 2488–2492; b) Y. Cui, J.-T. Chen, D.-L. Long, F.-K. Zheng, W.-D. Cheng, J.-S. Huang, *J. Chem. Soc. Dalton Trans.* **1998**, 2955–2956; c) T.-Y. Li, D.-Z. Liao, Z.-H. Jiang, G.-L. Wang, *Acta Chim. Sinica* **1996**, *54*, 679–684.

[6] a) J.-P. Costes, F. Dahan, A. Dupuis, J.-P. Laurent, *Inorg. Chem.* **1996**, *35*, 2400–2402; b) J.-P. Costes, F. Dahan, A. Dupuis, J.-P. Laurent, *Inorg. Chem.* **1997**, *36*, 3429–3433; c) J.-P. Costes, F. Dahan, A. Dupuis, J.-P. Laurent, *New J. Chem.* **1998**, *22*, 1525–1529; d) J.-P. Costes, F. Dahan, A. Dupuis, *Inorg. Chem.* **2000**, *39*, 165–168; e) J.-P. Costes, F. Dahan, G. Novitchi, V. Arion, S. Shova, J. Lipkowski, *Eur. J. Inorg. Chem.* **2004**, 1530–1537; f) R. Gheorghe, M. Andruh, J.-P. Costes, B. Donnadieu, *Chem. Commun.* **2003**, 2778–2779; g) G. Novitchi, S. Shova, A. Caneschi, J.-P. Costes, M. Gdaniec, N. Stanica, *Dalton Trans.* **2004**, 1194–1200; h) J.-P. Costes, F. Dahan, W. Wernsdorfer, *Inorg. Chem.* **2006**, *45*, 5–7; i) V. Tangoulis, J.-P. Costes, *Chem. Phys.* **2007**, *334*, 77–84.

[7] a) F. He, M.-L. Tong, X.-M. Chen, *Inorg. Chem.* **2005**, *44*, 8285–8292; b) X.-P. Yang, R. A. Jones, R. J. Lai, A. Waheed, M. M. Oye, A. L. Holmes, *Polyhedron* **2006**, *25*, 881–887.

[8] a) R. Koner, G. Lee, Y. Wang, H.-H. Wei, S. Mohanta, *Eur. J. Inorg. Chem.* **2005**, 1500–1505; b) S. Akine, T. Matsumoto, T. Taniguchi, T. Nabeshima, *Inorg. Chem.* **2005**, *44*, 3270–3274; c) M. Ryazanov, V. Nikiforov, F. Lloret, M. Julve, N. Kuzmina, A. Gleizes, *Inorg. Chem.* **2002**, *41*, 1816–1823; d) A. M. Atria, Y. Moreno, E. Spodine, M. T. Garland, R. Baggio, *Inorg. Chim. Acta* **2002**, *335*, 1–6; e) M. Sasaki, H. Horiuchi, M. Kumagai, M. Sakamoto, H. Sakiyama, Y. Nishida, Y. Sadaoka, M. Ohba, H. Okawa, *J. Chem. Soc. Dalton Trans.* **2000**, 259–263.

[9] a) X.-M. Chen, S. M. J. Aubin, Y.-L. Wu, Y.-S. Yang, T. C. W. Mak, D. N. Hendrickson, *J. Am. Chem. Soc.* **1995**, *117*, 9600–9601; b) X.-M. Chen, Y.-L. Wu, R.-J. Wang, *Science China, Ser. B* **1996**, *39*, 536–545; c) X.-M. Chen, Y.-L. Wu, Y.-X. Tong, X.-Y. Huang, *J. Chem. Soc. Dalton Trans.* **1996**, 2443–2448.

[10] a) Y.-Y. Yang, Y.-L. Wu, L.-S. Long, X.-M. Chen, *J. Chem. Soc. Dalton Trans.* **1999**, 2005–2009; b) X.-M. Chen, Y.-L. Wu, Y.-Y. Yang, S. M. J. Aubin, D. N. Hendrickson, *Inorg. Chem.* **1998**, *37*, 6186–6191; X.-M. Chen, M.-L. Tong, Y.-L. Wu, Y.-J. Luo, *J. Chem. Soc. Dalton Trans.* **1996**, 2181–2182.

[11] R. E. P. Winpenny, *Chem. Soc. Rev.* **1998**, *27*, 447–452.

[12] S.-P. Yang, L.-S. Long, X.-M. Chen, L.-N. Ji, *Acta Crystllogr. Sect. C* **1999**, *55*, 869–871.

[13] Y.-Y. Yang, PhD Thesis, Sun Yat-Sen (Zhongshan) University, **2001**.

[14] a) O. Kahn, *Molecular Magnetism*, VCH, Weinheim, **1993**; b) R. L. Carlin, *Magnetochemistry*, Springer, Berlin, **1986**.

[15] J. P. Sutter, M. L. Kahn, "Lanthanide Ions in Molecular Exchange Coupled Systems" in *Magnetism: Molecules to Materials* (Eds.: J. S. Miller, M. Drillon), **2004**, vol. 5, ch. 5, pp. 161–187.

[16] R. Gheorghe, P. Cucos, M. Andruh, J. Costes, B. Donnadieu, S. Shova, *Chem. Eur. J.* **2006**, *12*, 187–203.

[17] A. C. T. North, D. C. Phillips, F. S. Mathews, *Acta Crystallogr. Acta Crystallogr. Sect. A* **1968**, *24*, 351–359.

[18] G. M. Sheldrick, *SHELXTL-Plus*, Siemens Analytical X-ray Instruments Inc., Madison, WI, **1990**.

[19] G. M. Sheldrick, *SHELXL-97: Program for X-ray Crystal Structure Refinement*, Göttingen University, Germany, **1997**.

[20] *International Tables for X-ray Crystallography*, Vol. C, Tables 4.2.6.8 and 6.1.1.4, Kluwer Academic, Dordrecht, **1992**.

Received: September 25, 2007
Published Online: January 2, 2008

